BIOCHEMISTRY
including biophysical chemistry & molecular biology
Article

Biochemistry **2010,** *49,* 9217–9225 9217
DOI: 10.1021/bi1009858

Dynamic Regulation of Fibrinogen: Integrin αIIbβ3 Binding†

Roy R. Hantgan,*,‡ Mary C. Stahle,‡ and Susan T. Lord§

‡*Department of Biochemistry, Wake Forest University School of Medicine, Medical Center Boulevard, Winston-Salem, North Carolina 27157-1016, and* §*Department of Pathology and Laboratory Medicine, University of North Carolina, Chapel Hill, North Carolina 27599*

Received June 18, 2010; Revised Manuscript Received September 7, 2010

ABSTRACT: This study demonstrates that two orthogonal events regulate integrin αIIbβ3's interactions with fibrinogen, its primary physiological ligand: (1) conformational changes at the αIIb−β3 interface and (2) flexibility in the carboxy terminus of fibrinogen's γ-module. The first postulate was tested by capturing αIIbβ3 on a biosensor and measuring binding by surface plasmon resonance. Binding of fibrinogen to eptifibatide-primed αIIbβ3 was characterized by a k_{on} of ∼2×10^4 L mol^{-1} s^{-1} and a k_{off} of ∼8×10^{-5} s^{-1} at 37 °C. In contrast, even at 150 nM fibrinogen, no binding was detected with resting αIIbβ3. Eptifibatide competitively inhibited fibrinogen's interactions with primed αIIbβ3 ($K_i \sim 0.4$ nM), while a synthetic γ-module peptide (HHLGGAKQAGDV) was only weakly inhibitory ($K_i > 10$ μM). The second postulate was tested by measuring αIIbβ3's interactions with recombinant fibrinogen, both normal (rFgn) and a deletion mutant lacking the γ-chain AGDV sites (rFgn γΔ408−411). Normal rFgn bound rapidly, tightly, and specifically to primed αIIbβ3; no interaction was detected with rFgn γΔ408−411. Equilibrium and transition-state thermodynamic data indicated that binding of fibrinogen to primed αIIbβ3, while enthalpy-favorable, must overcome an entropy-dominated activation energy barrier. The hypothesis that fibrinogen binding is enthalpy-driven fits with structural data showing that its γ-C peptide and eptifibatide exhibit comparable electrostatic contacts with αIIbβ3's ectodomain. The concept that fibrinogen's αIIbβ3 targeting sequence is intrinsically disordered may explain the entropy penalty that limits its binding rate. In the hemostatic milieu, platelet−platelet interactions may be localized to vascular injury sites because integrins must be activated before they can bind their most abundant ligand.

Regulated fibrinogen binding to some 80000 αIIbβ3 integrins resident on human blood platelets is essential to normal hemostasis and aberrant in thrombosis (*1*, *2*). Despite their crucial role in human health and disease, defining the molecular mechanisms that shift αIIbβ3 from a quiescent heterodimer to a hemostatically active receptor remains a challenge (*3*−*6*). Recent evidence indicates that intracellular integrin activation involves talin binding to the β3 cytodomain, triggering subunit shifts that ultimately extend the ectodomain (*7*, *8*). Advances in structural biology also support outside-in signaling models in which subtle conformational changes linked to ligand binding at the αIIb β-propeller−β3 I domain interface (*6*, *9*, *10*) are allosterically coupled to rearrangements of the receptor's transmembrane segments and cytodomains (*11*−*14*). Pharmaceutical integrin ligands present a twist: they bind to resting αIIbβ3, but it then populates an active form that persists for hours after their dissociation (*15*, *16*).

While platelet stimulation is clearly prerequisite for fibrinogen binding, affinity estimates (K_d) for this abundant protein (plasma concentration of ∼10 μM) range from <100 nM (*17*−*19*) to >2 μM (*20*, *21*). Studies incorporating αIIbβ3 in lipid vesicles yielded K_d values from 5 to 15 nM (*22*−*24*), but uncertainty about the receptors' activation state raises new questions. Subsequent reports using solid-phase binding assays indicated that fibrinogen binds rapidly ($k_{on} \sim 8 \times 10^5$ L mol^{-1} s^{-1}) (*25*) and tightly ($K_d \sim$ 60 nM) (*26*) to immobilized αIIbβ3. However, those affinity-purified integrins were isolated by a process that selects for preactivated receptors (*27*, *28*), so binding regulation was not addressed. In contrast, Du et al. (*29*) demonstrated that αIIbβ3 acquired the ability to bind fibrinogen ($K_d \sim 50$ nM) following overnight incubation with, and then washout of, synthetic peptide GRGDSP or HHLGGAKQAGDV,[1] albeit at a large molar excess.

Biophysical studies subsequently revealed multistep fibrinogen binding kinetics and raised new questions. The pioneering surface plasmon resonance (SPR) studies of Huber et al. (*30*) illustrate a quandary. Their biosensor-immobilized integrins only reproducibly interacted with fibrinogen after several cycles of surface regeneration with an RGD peptide. That fits with our observation that RGD peptides shift the initially resting receptor to an open conformation (*31*). They reported a rapid initial on rate k_{on} of ∼3×10^5 L mol^{-1} s^{-1} and a K_d of 165 nM (*30*). Muller et al. (*32*) described total internal reflection fluorescence measurements with unstimulated αIIbβ3 reconstituted in lipid bilayers. They found a

†Supported by Grant-in-Aid 0855257E from the American Heart Association, Mid-Atlantic Affiliate (to R.R.H.), Institutional Development Grant 2006-IDG-1004 from the North Carolina Biotechnology Center (to R.R.H.), and Grant HL031048−22 from the National Institutes of Health (to S.T.L.).

*To whom correspondence should be addressed. Telephone: (336) 716-4675. Fax: (336) 716-7671. E-mail: rhantgan@wfubmc.edu.

[1]Abbreviations: HSCM, pH 7.4 buffer containing 0.13 mol/L NaCl, 0.01 mol/L HEPES, 0.001 mol/L $CaCl_2$ and 0.001 mol/L $MgCl_2$; HSCM-OG, HSCM buffer with 0.03 mol/L *n*-octyl-β-D-glucopyranoside; HSCM-T, HSCM buffer with 0.01% Tween; RU, response units; SPR, surface plasmon resonance; HHLGGAKQAGDV, synthetic peptide L-histidiyl-L-histidyl-L-leucyl-glycyl-glycyl-L-alanyl-L-lysyl-L-glutamyl-L-alanyl-gylcyl-L-aspartyl-L-valine.

Published on Web 09/09/2010

slower k_{on} of $\sim 4 \times 10^4$ L mol^{-1} s^{-1}, for the initial binding event but a smaller K_d of ~50 nM; slower formation of an irreversible complex followed. In contrast, Pesho et al. (*33*) fit their SPR data to a 1:1 binding model for fibrinogen's interactions with RGD-purified αIIbβ3 covalently coupled to biosensors. They obtained a k_{on} of $\sim 3 \times 10^5$ L mol^{-1} s^{-1} and a much tighter K_d of ~3 nM. To resolve the relationship between integrin activation and the rate or affinity of fibrinogen binding, we purified αIIbβ3 in a resting conformation (*34*) that can be modulated by transient exposure to a priming ligand prior to delivery of a macromolecule for SPR binding studies (*16*).

The fibrinogen $(A\alpha B\beta\gamma)_2$ molecule is rich in potential integrin recognition sites, with classic RGD sequences midway through the α-chains' coiled-coil regions and on their carboxy-terminal segments. However, fibrinogen molecules with RGE substitutions at Aα 95−97 or Aα 572−574 supported aggregation of ADP-stimulated platelets as effectively as plasma fibrinogen (*35*) or normal recombinant fibrinogen (*36*). Fibrinogen's γ-chains also have a unique αIIbβ3 targeting sequence, HHLGGAKQAGDV (*37*, *38*). The plasma fibrinogen variant $(A\alpha B\beta\gamma')$-$(A\alpha B\beta\gamma)$, which lacks that sequence on one of its γ-chains, exhibited only half-maximal activity in platelet aggregation and fibrinogen binding assays (*35*, *39*). Likewise, recombinant $(A\alpha B\beta\gamma')_2$ showed a markedly decreased level of platelet binding (*40*), and a recombinant fibrinogen variant with its γ-chain AGDV sites deleted (rFgn γΔ408−411) failed to support platelet aggregation (*36*, *41*). In contrast, another recombinant fibrinogen variant with dysfunctional α-chain RGE sites and deleted γ-chain AGDV sites exhibited substantial clot retraction (*36*). Auxiliary integrin-binding sites localized to γ316−322 (*42*−*44*) and γ370−381 (*45*, *46*) may play special roles in mediating the adhesion of platelets to immobilized fibrinogen and clotted fibrin.

While these observations strongly suggest that αIIbβ3−fibrin(ogen) interactions are mediated not by its RGD sites but rather by residues present on its γ-module, this concept has not been rigorously tested in a purified system. Here, we present evidence from SPR measurements performed with recombinant fibrinogen, both normal and rFgn γΔ408−411, that residues on the carboxy terminus of its γ-module are essential for tight binding to primed αIIbβ3. Combining our equilibrium and transition-state thermodynamic data with structural insights, we propose a new model for the dynamic regulation of integrin−fibrinogen interactions.

EXPERIMENTAL PROCEDURES

αIIbβ3 Purification. Milligram quantities of highly purified αIIbβ3 were isolated from outdated human blood platelets (Blood Bank, North Carolina Baptist Hospital, Winston-Salem, NC) by affinity and size-exclusion chromatography in HSCM-OG buffer as previously described (*47*).

Anti-αIIb Cytodomain IgG. Antibody A4 was isolated by affinity chromatography from the serum of rabbits immunized with a synthetic peptide, L-cysteinyl-L-prolyl-L-leucyl-L-glutamyl-L-glutamyl-L-aspartyl-L-aspartyl-L-glutamyl-L-glutamyl-glycyl-L-glutamic acid, corresponding to the 10 carboxy-terminal residues of the αIIb cytoplasmic domain as previously described (*16*).

Integrin Antagonists. COR Therapeutics (San Francisco, CA) provided eptifibatide [Integrilin; N^6-(aminoiminomethyl)-N^2-(3-mercapto-1-oxopropyl-L-lysylglycyl-L-α-aspartyl-L-tryptophanyl-L-prolyl-cysteinamide, cyclic [1−6]-disulfide]. It was used at concentrations, determined spectrally, that yielded >80% receptor saturation (*15*). Synthetic peptide L-histidiyl-L-histidyl-L-leucyl-glycyl-glycyl-L-alanyl-L-lysyl-L-glutamyl-L-alanyl-gylcyl-L-aspartyl-L-valine (HHLGGAKQAGDV) was prepared and characterized by the Protein Analysis Core Laboratory of the Comprehensive Cancer Center of Wake Forest University; peptide concentrations were determined by amino acid analysis.

Fibrinogen. Highly purified human fibrinogen, free of plasminogen and Factor XIII, was purchased from American Diagnostica (Stamford, CT). Following reconstitution in HSCM buffer and extensive dialysis, fibrinogen concentrations were determined spectrally (*48*).

Recombinant Fibrinogens. Normal and γΔ408−411 recombinant fibrinogens were synthesized in CHO cells as described previously (*41*, *49*). Cells were cultured in roller bottles by Biovest International Inc./NCCC (Minneapolis, MN). Serum-free medium containing secreted fibrinogen was harvested periodically; protease inhibitors were added, and the medium was stored at −20 °C prior to being shipped on dry ice. Recombinant fibrinogen was purified as described previously (*41*, *49*). Briefly, fibrinogen was precipitated from the medium with ammonium sulfate in the presence of a cocktail of protease inhibitors. The precipitate was resuspended in buffer containing 10 mM $CaCl_2$ and applied to a Sepharose 4B column coupled with the fibrinogen-specific monoclonal antibody, IF-1. Fibrinogen was eluted from the column with buffer containing 5 mM EDTA, dialyzed against HBS [20 mM HEPES (pH 7.4) and 150 mM NaCl] and 1 mM $CaCl_2$ for one exchange, then extensively dialyzed against HBS, and stored at −80 °C. The integrity of the polypeptide chains and the purity of the recombinant protein were analyzed by SDS−PAGE under reduced and nonreduced conditions.

Surface Plasmon Resonance Spectroscopy. Measurements were performed in a Biacore T100 instrument by monitoring the changes in response units (RU) at the biosensor surface (*47*). Signals from both the reference and sample channels were collected at a rate of 10 Hz. Reagents were maintained at 25.0 ± 0.1 °C in the sample compartment; data were collected at 37, 25, or 15 °C with control to ±0.01 °C in the analysis chamber.

Purified A4 IgG, specific for the integrin αIIb carboxy-terminal segment, was covalently coupled to the sample and reference cells of CM-5 chips to achieve a surface density of 10000−12000 RU, followed by ethanolamine blocking (*16*). Most experiments used primed integrins, delivered to the sample channel at 530 ± 120 nM (n = 16) in HSCM-OG in the presence of a 6-fold molar excess of eptifibatide. In selected experiments, resting integrins at 370 ± 170 nM (n = 2) were captured in HSCM-OG. Following the initial capture step, samples were stabilized for 20 min, while HSCM-T buffer flowed over the chip. Note that this step removed the octyl glucoside and priming agent (*16*). Similar capture levels resulted at 37 °C with primed (300 ± 150 RU; n = 12) and resting integrins (124 ± 59 RU; n = 2). Increased levels were obtained with primed receptors at lower temperatures: 502 ± 47 RU (n = 2) at 25 °C and 514 ± 58 RU (n = 2) at 15 °C. To correct for differences in capture levels, fibrinogen binding signals were normalized by the integrin capture RU for each cycle.

At each temperature, one or two start-up cycles were performed: a midrange fibrinogen concentration (40−50 nM in HSCM-T) was delivered to the sample and reference channels, followed by a two-step regeneration cycle, first with 3 M NaCl and then with pH 3 glycine buffer. Next, during the binding steps, an aliquot of fibrinogen (0−150 nM) was delivered to both flow cells at a rate of 20 μL/min for 1000 s; dissociation of the

integrin−fibrinogen complexes was then monitored for 1500 s, as HSCM-T buffer flowed over the biosensor surface at a rate of 30 μL/min. The biosensor was regenerated and equilibrated for 300 s with buffer prior to the next cycle.

Representative RU versus time profiles depicting integrin capture, stabilization, fibrinogen binding (or buffer blank), and regeneration are presented in Figure S1 of the Supporting Information. Note that αIIbβ3 bound rapidly (k_{on} = 1.7 × 10^4 L mol^{-1} s^{-1}) to immobilized mAb A4 and then dissociated slowly (k_{off} = 2.5 × 10^{-5} s^{-1}) during the stabilization period. The doubly corrected signals noted earlier account for integrin dissociation effects.

SPR Kinetic Analyses. Sensorgram responses, the difference in RU versus time between sample and reference channels at each fibrinogen concentration, were further corrected by subtraction of profiles obtained with a buffer blank. These doubly corrected signals (*50*) were then fit globally by nonlinear regression (Biacore evaluation software) to a 1:1 binding model (*47*). The quality of the fits was judged by the residuals as well as the signal-to-noise ratio ($\langle RU \rangle / \sqrt{\chi^2}$). As described in Table S1 of the Supporting Information, we also explored fitting each data set to a bivalent analyte model, which did not significantly improve the goodness of fit. Table S2 of the Supporting Information shows other analyses that validate the off-rate determinations.

Reasoning that any effects of multisite binding would be minimized at lower integrin capture densities, we conducted a series of fibrinogen binding experiments at input concentrations of primed αIIbβ3 of 251, 125, and 61 nM, yielding integrin capture levels of 276, 147, and 48 RU, respectively. As illustrated in Figure S2 of the Supporting Information, comparable binding and dissociation kinetic profiles resulted at each integrin density. While lower fibrinogen binding levels were observed at lower integrin capture levels, each data set was described well by a 1:1 binding model. The finding that both the forward and reverse rate constants for fibrinogen−integrin interactions were essentially independent of the integrin capture level, over a 6-fold range, indicates that multivalent interactions do not make a significant contribution to complex formation in our system. Hence, we used the 1:1 binding model for all kinetic analyses in this work.

Solid-Phase Binding Assays. αIIbβ3 (34 μg/mL, 150 nM), either resting or primed by incubation with 2 μM eptifibatide for 2 h at 37 °C, in HSCM-OG was coupled to Pierce Reacti-Bind Amine-Binding Maleic Anhydride 96-well plates and incubated overnight at 4 °C. Fibrinogen was derivatized with EZ-Link-Sulfo-NHS-biotin (Pierce) in a 2 h reaction in PBS at 0 °C followed by extensive dialysis at room temperature. The degree of labeling, 7.3 mol of biotin/mol of protein, was determined by difference spectroscopy using an avidin displacement assay (Pierce). Biotinylated fibrinogen samples (0−30 nM) were incubated in integrin-coated or buffer blank wells for 1 h at room temperature, followed by washing and color development steps as previously described (*16*).

RESULTS

Binding of Fibrinogen to Resting and Primed αIIbβ3. SPR kinetic data demonstrated that fibrinogen bound rapidly and tightly to primed, but not resting, αIIbβ3 receptors immunocaptured on a biosensor (Figure 1A). Fitting the data obtained with primed αIIbβ3 and fibrinogen (5−150 nM) to a 1:1 binding model (eq 1) yielded a close correspondence between the data

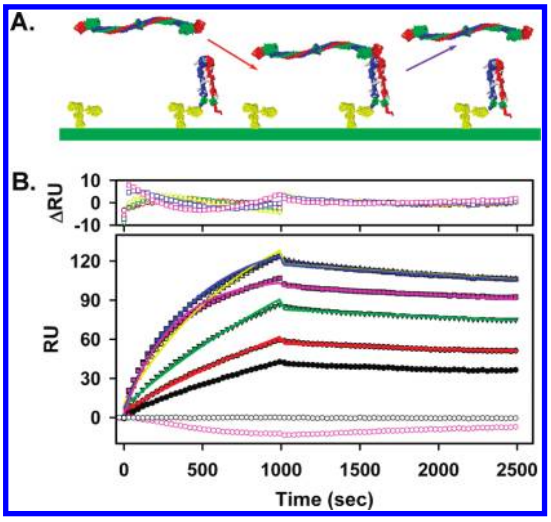

FIGURE 1: Kinetics of binding of fibrinogen to αIIbβ3 determined by surface plasmon resonance. (A) Schematic of integrin immunocapture on a biosensor surface, followed by reversible fibrinogen binding. (B) SPR kinetic traces depicting the time course of concentration-dependent binding of fibrinogen to eptifibatide-primed αIIbβ3. The following fibrinogen concentrations were used: 5 (black), 10 (red), 20 (green), 50 (yellow), 100 (blue), and 150 nM (pink). The weakened signals at 100 and 150 nM fibrinogen were caused by less efficient integrin capture in the later cycles of this experiment. Solid lines were determined by fitting the data to a 1:1 reversible binding model; residuals are shown in the top panel. The fitting routine also has a term that accounts for the small, sharp drop in RU at the start of the dissociation step. This effect is due to a slight difference in the refractive index in sample vs running buffer. No fibrinogen binding was detected with resting αIIbβ3 [empty symbols for 5 (black) and 150 nM (pink); data from other concentrations omitted for the sake of clarity]. All data were collected at 37 °C.

(Figure 1B, filled symbols) and fitted lines as well as a narrow distribution of residuals.

$$\text{Fgn} + \alpha\text{IIb}\beta3 \underset{k_d}{\overset{k_a}{\rightleftarrows}} \alpha\text{IIb}\beta3\text{−Fgn} \qquad (1)$$

This analysis resulted in a k_a of (2.19 ± 0.01) × 10^4 L mol^{-1} s^{-1}, a k_d of (7.01 ± 0.04) × 10^{-5} s^{-1}, and a dissociation constant (K_d = k_d/k_a) of 3.20 × 10^{-9} M for binding of fibrinogen to primed αIIbβ3 at 37 °C. In contrast, only negative RU versus time profiles resulted with resting receptors (Figure 1B, empty symbols), indicating no detectable interactions even at 150 nM fibrinogen.

These findings were confirmed with a solid-phase binding assay in which biotinylated fibrinogen (0−30 nM) was incubated with resting or primed αIIbβ3 covalently coupled to the wells of a microtiter plate (*16*). Fibrinogen exhibited a hyperbolic, saturable binding profile with the primed receptor, characterized by a 2.0 ± 0.4 nM midpoint. In contrast, signals obtained with resting integrins exhibited a shallow, linear dependence on fibrinogen concentration. These data indicate that fibrinogen binds ~100-fold more tightly to primed, compared to resting, integrins (Figure S3 of the Supporting Information).

Blocking Binding of Fibrinogen to Primed αIIbβ3. Next, we investigated the paradox that eptifibatide, the integrin antagonist that we used to prime αIIbβ3 here and in our previous studies with PAC-1(*16*), also inhibits binding of fibrinogen to its platelet receptors (*51*). SPR kinetic data demonstrated that delivering fibrinogen (100 nM) in the presence of eptifibatide (10 nM) weakened the binding signal 5-fold compared to a control; 100 nM eptifibatide resulted in near-complete binding inhibition (Figure 2). These data are presented as the ratio of the

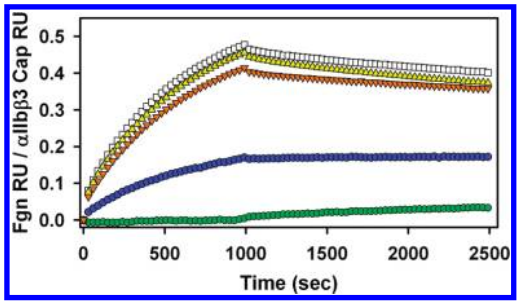

FIGURE 2: Inhibition of binding of fibrinogen to αIIbβ3 by eptifibatide and HHLGGAKQAGDV γC peptide. To facilitate comparison between experiments, SPR kinetic traces are presented as the ratio of the fibrinogen binding signals to those for αIIbβ3 immunocapture: (empty squares) 100 nM fibrinogen binding control, (yellow triangles) 100 nM fibrinogen and 300 nM γC peptide, (orange triangles) 100 nM fibrinogen and 3000 nM γC peptide, (blue circles) 100 nM fibrinogen and 10 nM eptifibatide, and (green circles) 100 nM fibrinogen and 100 nM eptifibatide. All data were collected at 37 °C.

fibrinogen binding RU signal to the αIIbβ3-captured RU signal to facilitate comparison between experiments.

Analysis of the complete data set with a competitive inhibition model demonstrated eptifibatide (10−1000 nM) reduced the level of fibrinogen binding by 50% at a mole ratio of 0.08 ± 0.03 (Figure S4 of the Supporting Information). This result indicates that eptifibatide binds ~10-fold tighter than fibrinogen to αIIbβ3. These findings were confirmed with a solid-phase binding assay that demonstrated that eptifibatide (2 μM) reduced the level of fibrinogen binding (0−30 nM) to near-background levels (Figure S4 of the Supporting Information). We conclude that eptifibatide's ability to bind tightly to αIIbβ3 (*15*), shifting it from a resting to a ligand-competent conformation (*16*, *52*), and then to dissociate rapidly (*16*) contributes to its ability to both promote and block binding of fibrinogen to αIIbβ3.

Given the importance of the carboxy terminus of fibrinogen's γ-module in promoting interactions with αIIbβ3 (*10*, *53*, *54*), we investigated the ability of a synthetic peptide spanning that sequence to block binding of fibrinogen to primed αIIbβ3. SPR kinetic data demonstrated that peptide HHLGGAKQAGDV was a weak inhibitor, reducing the magnitude of the fibrinogen binding signal by <10% at 3 μM, a 30-fold molar excess (Figure 2 and Figure S4 of the Supporting Information). This observation fits with the findings of Kloczewiak et al. (*55*), who first developed a series of γC peptides as platelet-aggregation inhibitors. They reported an IC_{50} of 28 μM (165-fold molar excess) for HHLGGAKQAGDV inhibition of binding of [^{125}I]-fibrinogen to human platelets; maximal inhibition of platelet aggregation required 60 μM peptide (*55*). Because conformational flexibility could limit this synthetic ligand's effectiveness, we also measured αIIbβ3's interactions with a recombinant fibrinogen variant lacking critical residues in its γ-module.

Recombinant Fibrinogen Binding to Primed αIIbβ3. SPR demonstrated that normal recombinant fibrinogen (Figure 3A, filled symbols) bound rapidly and tightly to immunocaptured, eptifibatide-primed αIIbβ3 at 37 °C. Fitting the kinetic data obtained in three experiments with normal rFgn (10, 20, 25, 30, 60, 100, 125, and 150 nM) to a 1:1 binding model (eq 1) yielded the solid lines in Figure 3A. The resultant kinetic parameters [$k_a = (2.19 \pm 0.01) \times 10^4$ L mol^{-1} s^{-1}, $k_d = (3.94 \pm 0.01) \times 10^{-5}$ L mol^{-1} s^{-1}, and $K_d = 1.80 \times 10^{-9}$ M] are comparable to those obtained with highly purified human plasma fibrinogen (Figure 1). In contrast, no binding signals were detected with rFgn $\gamma\Delta$408−411, even at 100 nM (Figure 3A, empty symbols).

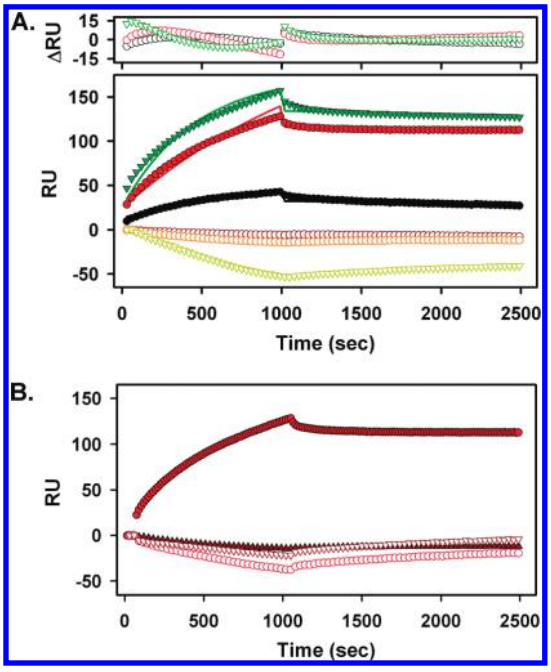

FIGURE 3: Kinetics of binding of recombinant fibrinogen to primed αIIbβ3 determined by surface plasmon resonance. (A) SPR kinetic traces depicting the time course of concentration-dependent binding of normal recombinant fibrinogen (10, 30, and 100 nM) to eptifibatide-primed αIIbβ3 (filled symbols). Solid lines were determined by global fitting of the complete data set (three experiments and eight fibrinogen concentrations) to a 1:1 reversible binding model; residuals are shown in the top panel. No binding was detected with rFgn $\gamma\Delta$408−411 (empty symbols). All data were collected at 37 °C. (B) SPR kinetic traces showing eptifibatide inhibition of binding of recombinant fibrinogen to primed αIIbβ3. Normal recombinant fibrinogen (30 nM, red circles) and eptifibatide (26 μM, empty circles). Note the complete inhibition. rFgn $\gamma\Delta$408−411 (30 nM, dark red triangles) and eptifibatide (26 μM, empty triangles). Note the similar negative RU traces in both cases.

Excess eptifibatide fully blocked normal rFgn binding, reducing the time-dependent RU traces to the background levels observed with rFgn $\gamma\Delta$408−411 (Figure 3B). Note that excess eptifibatide had little effect on the near-baseline RU signals obtained with this mutant. Taken together, the observations in Figure 3 indicate that both plasma and recombinant fibrinogens use similar mechanisms to bind primed αIIbβ3 with similar specificity.

Temperature Dependence of αIIbβ3−Fibrinogen Binding. Measuring the temperature dependence of binding of fibrinogen to primed αIIbβ3 provided additional insights into the mechanisms that regulate these interactions. Figure 4 presents SPR kinetic traces obtained at 37, 25, and 15 °C with plasma fibrinogen; data are presented as the ratio of the fibrinogen-bound to integrin-capture RU signals to facilitate comparisons. Binding specificity was confirmed with blocking experiments performed at 100 nM fibrinogen and 20 μM eptifibatide, which reduced the signal below background levels at each temperature.

The solid lines in each panel were obtained by a global fit of data obtained in duplicate experiments to a 1:1 binding model to determine the on and off rate constants and, from them, the dissociation constant at each temperature. In each case, the narrow distribution of residuals confirms the validity of the fits. Data obtained at 37 °C yielded a k_a of (1.90 ± 0.01) × 10^4 L mol^{-1} s^{-1}, a k_d of (8.41 ± 0.03) × 10^{-5} s^{-1}, and a K_d of 4.42 × 10^{-9} mol/L. At 15 °C, the on rate was ~2-fold slower and the off

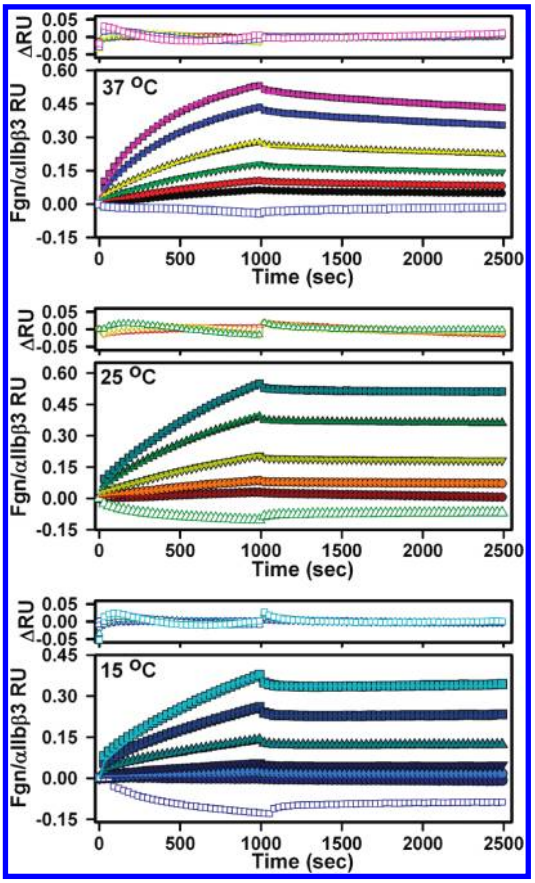

FIGURE 4: Temperature dependence of the kinetics of fibrinogen binding to primed αIIbβ3 determined by surface plasmon resonance. To facilitate comparison between experiments, SPR kinetic traces are presented as the ratio of the fibrinogen binding signals (5, 10, 20, 50, 100, and 150 nM) to those for αIIbβ3 immunocapture. Solid lines were determined by fitting the data in duplicate experiments to a 1:1 reversible binding model; residuals are presented in the top panels. The empty symbols denote the inhibitory effects of excess eptifibatide (26 μM) on binding of 100 nM fibrinogen.

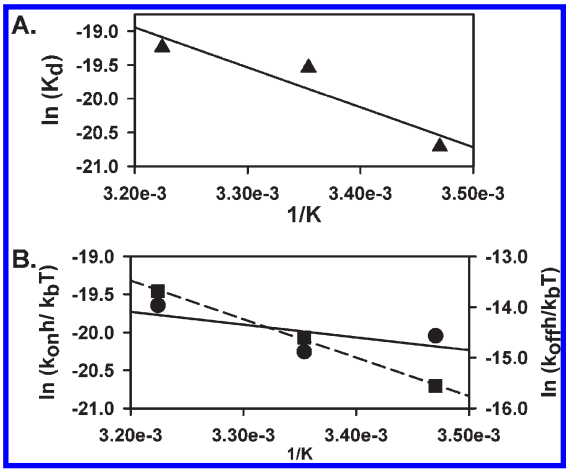

FIGURE 5: Equilibrium and transition-state thermodynamic analyses of binding of fibrinogen to primed αIIbβ3. (A) van't Hoff analysis of the temperature dependence of the equilibrium dissociation constants for αIIbβ3−fibrinogen complexes. The solid line was determined by linear regression. Enthalpy ($\Delta H°$) and entropy ($\Delta S°$) changes for αIIbβ3−fibrinogen binding were determined from the regression line's slope and intercept, respectively (*47*). (B) Eyring analysis of the temperature dependence of the forward and reverse rate constants for αIIbβ3−fibrinogen complexes. Data are presented as the logarithm of the association rate, k_a data, divided by the kelvin temperature, and scaled by the ratio of Planck's constant, h, to Boltzmann's constant, k_b, plotted vs $1/T$ (●). The activation enthalpy ($\Delta H_a^{\circ\ddagger}$) and entropy ($\Delta S_a^{\circ\ddagger}$) were calculated from the slope and intercept, respectively, of the solid line, determined by linear regression, as described previously (*47*). Analogous procedures for the dissociation rate constant, k_d (■ with dashed line), yielded $\Delta H_d^{\circ\ddagger}$ and $\Delta S_d^{\circ\ddagger}$.

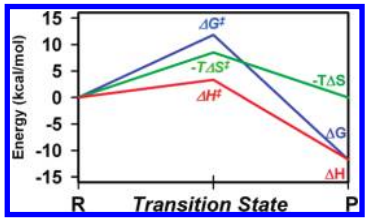

FIGURE 6: Free energy profile for αIIbβ3−fibrinogen complexes. Changes in free energy, enthalpy, and entropy are depicted along the path from reactants to products. Note that binding requires overcoming an entropy-dominated transition-state barrier before an enthalpy-stabilized receptor−ligand complex is reached.

rate ~7-fold slower, yielding ~4-fold tighter binding at the lower temperature. Intermediate values were obtained at 25 °C.

Equilibrium and Transition-State Thermodynamic Data for αIIbβ3−Fibrinogen Binding. A van't Hoff plot (*47*, *56*) of the temperature dependence of K_d, determined from the ratio of the reverse and forward rate constants at each temperature, yielded a negative slope and a near-zero intercept (Figure 5A). The resultant equilibrium thermodynamic parameters indicated fibrinogen binding is enthalpy-driven, characterized by a $\Delta H°$ of -11.7 ± 4.4 kcal/mol and a $\Delta S°$ of ~0. Following Eyring's reaction rate formalism (*47*, *57*), plotting the temperature dependence of the rate constants (Figure 5B) yielded a set of transition-state thermodynamic parameters. This analysis demonstrated that the transition-state free energy barrier ($\Delta G^{\circ\ddagger} = 11.8 \pm 5.2$ kcal/mol) is dominated by an unfavorable activation entropy ($\Delta S^{\circ\ddagger} = -28.5 \pm 12.5$ cal K^{-1} mol^{-1}) while the enthalpic contribution ($\Delta H^{\circ\ddagger}$) approaches 0. These points are summarized in the reaction coordinate diagram presented in Figure 6.

DISCUSSION

Integrin Antagonist Priming Mechanisms. αIIbβ3 normally resides in a quiescent conformation (*31*, *34*, *58*) rendered inaccessible to macromolecular ligands by an activation energy barrier ($\Delta G^{\circ\ddagger} > 10$ kcal/mol) (*16*). In contrast, pharmaceutical integrin antagonists readily bind to the resting integrin and shift the equilibrium toward a primed conformer that remains populated at least 90 min post-receptor occupancy (*15*, *16*). In this work, we showed how this conformational hysteresis provides a window for avid fibrinogen binding.

Thanks to recent X-ray diffraction crystallographic structures of integrins, we can consider molecular mechanisms that may explain our observations. Structural data for αIIbβ3's resting ectodomain (Protein Data Bank entry 3FCS) (*6*) as well as complexes with eptifibatide (Protein Data Bank entry 2VDN) (*6*, *9*) and fibrinogen's γ-C peptide (Protein Data Bank entry 2VDO) (*10*) provide insights into subtle rearrangements that accompany ligand binding at the interface between αIIb's β-propeller and β3's I domain. As illustrated in Figure 7, both these ligands occupy similar positions when bound to the αIIbβ3 ectodomain. The overall size of αIIbβ3's ligand-binding pocket, measured as the distance between the MIDAS Mg^{2+} and the salt-bridging carboxylate anion on αIIb D224, was 19.9 Å in the resting ectodomain, 19.5 Å with eptifibatide bound, and 19.7 Å

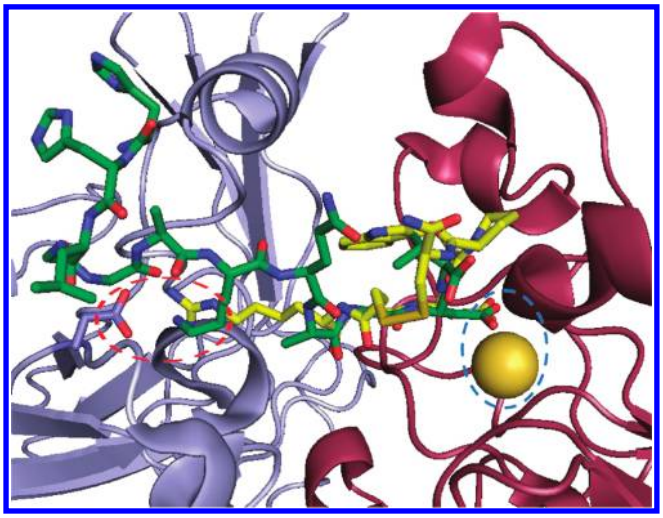

FIGURE 7: Integrin−ligand binding modes. Fibrinogen's γC peptide (green backbone) and eptifibatide (yellow backbone) occupy similar positions in αIIbβ3's ligand-binding crevice. αIIb and β3 polypeptides are shown as blue and red ribbons, respectively; highlighted atoms shown in ball-and-stick representation are color-coded as follows: red for oxygen and blue for nitrogen. In both cases, a ligand aspartate forms an electrostatic contact with the β3 subunit's MIDAS Mg^{2+} (highlighted by the blue-dashed ellipse). Additional stabilization is provided by a tight turn that enables the γC lysine's ζN^+ atom to form a salt bridge with a carboxylate anion on αIIb's Asp224; the ηN^+ atom on eptifibatide's homoarginine makes a similar contact (highlighted by a red-dashed ellipse). This figure was prepared with Pymol (*76*) and is based on crystal structure data presented by Springer et al. (*10*) for complexes formed between αIIbβ3's ectodomain and fibrinogen's γC peptide (Protein Data Bank entry 2VDO) and eptifibatide (Protein Data Bank entry 2VDN).

with HHLGGAKAQGDV bound. Because even the resting receptor's pocket appears to be sufficiently large to fit the γ-C peptide, whose zwitterions are separated by only 17 Å, we must consider other factors to understand how fibrinogen binding is regulated.

Using the metal ion-dependent adhesion site (MIDAS) as a reference, we find that ligand binding shifts the adjacent Ca^{2+} ion in the AdMIDAS site, considered a negative regulator of adhesiveness (*59*), some 2−3 Å closer to the MIDAS Mg^{2+}. Perhaps more importantly, that Ca^{2+} moves within ~4 Å of the carboxylate anion on β3 residue D251, a distance that allows electrostatic interactions (*60*). As Zhu et al. (*6*) demonstrated, the net increased positive charge on the MIDAS Mg^{2+} now favors strong ionic interactions with aspartate carboxylates that reside ~3 Å away on both eptifibatide and fibrinogen's γ-C peptide.

While these conformational changes are likely to be readily reversible, they are linked to larger polypeptide chain rearrangements initiated by downward movement of β3's α7 helix and swing-out of its hybrid domain (*9*). Allosteric propagation through β3's hybrid and PSI domains disrupts contacts with αIIb's thigh domain, eventually leading to an extended integrin with a gap between its transmembrane and cytoplasmic domains (*11*). We propose that the substantial conformational changes that characterize this maximally activated integrin (*14*) may well account for the metastable, integrin-antagonist primed state that binds fibrinogen (this work) and PAC-1 (*16*), each with nanomolar affinity.

Factors Limiting the On and Off Rates of the Fibrinogen−αIIbβ3 Complex. We demonstrated that fibrinogen binds rapidly to eptifibatide-primed αIIbβ3 ($k_a \sim 2 \times 10^4$ L mol^{-1} s^{-1} at 37 °C). However, this process is ~70-fold slower than the initial step in forming an activated integrin−PAC-1 complex (*16*), which raises a question. What factors limit fibrinogen binding? Structural data indicate that both macromolecular ligands recognize αIIbβ3 through similar zwitterionic interactions (*10*, *61*). While PAC-1's RYD sites reside on a loop on the IgM's Fab domains (*61*, *62*), the integrin targeting sequence at the carboxy terminus of fibrinogen's γC module exhibited no discernible electron density in crystal structures of human fibrinogen (*63*), fragment D-dimer (*64*), or recombinant fragment D (*65*). These observations suggest that the γ-chain segment on fibrinogen is highly flexible (*63*, *66*) and possibly intrinsically disordered (*10*).

In contrast, when bound to the αIIbβ3 ectodomain, synthetic HHLGGAKQAGDV displays a unique structure (*10*), characterized by a tight turn that positions its lysine's ζN^+ atom within 3 Å of a carboxylate anion on αIIb's Asp224 (Figure 7). The ligand's aspartate is likewise within 3 Å of the β3 MIDAS Mg^{2+}, providing a key source of stability. Indeed, our studies with rFgn $\gamma\Delta$408−411 clearly confirm that this electrostatic contact is an essential feature of the αIIbβ3−fibrinogen complex. The contrast between the tightly structured γC peptide−αIIbβ3 ectodomain complex and fibrinogen's flexible γ-chain carboxy terminus may explain our observation that the activation free energy barrier between reactants and products is dominated by an unfavorable entropy term (Figure 6). We propose that the conformational entropy cost of transition-state formation strongly contributes to the relatively slow rate of integrin−fibrinogen binding.

Once bound, fibrinogen dissociates quite slowly from the primed αIIbβ3 receptor, exhibiting a decay time of ~200 min at 37 °C, some 70-fold slower than that of eptifibatide (*16*). On the basis of our experience studying αIIbβ3's interactions with pentameric PAC-1 (*16*), we recognized that these rather slow off rates might be due to multivalent interactions with fibrinogen, a covalent $(A\alpha B\beta\gamma)_2$ homodimer with an integrin targeting sequence on each of its distal γ-modules. In their classic study of the interactions between human growth hormone and its receptor's extracellular binding domain, Cunningham and Wells (*67*) demonstrated by SPR that blocking formation of dimeric receptor−ligand complexes increased the dissociation rate constant from $< 10^{-5}$ to $\sim 4 \times 10^{-4}$ s^{-1}. Similarly, Duan et al. (*68*) reported minimal dissociation for a pentameric monobody bound to the αvβ3 integrin, while a single-domain construct dissociated at least 100-fold faster. However, our fibrinogen binding kinetic data were not influenced by the integrin capture level (Figure S2 of the Supporting Information), and fitting them to a bivalent analyte model yielded no significant improvement in the goodness of fit (Table S1 of the Supporting Information); therefore, we conclude that fibrinogen binding to multiple immobilized integrins did not make a significant contribution to our findings.

Alternatively, several lines of evidence indicate that while fibrinogen shares a zwitterionic binding motif with eptifibatide (*10*), its macromolecular multidomain structure provides additional binding sites that may stabilize its complex with αIIbβ3. In addition to fibrinogen's primary integrin-recognition motif, γ400−411, auxiliary integrin binding sites have been localized to γ316−322 (*42*−*44*) and γ370−381 (*45*, *46*). Likewise, mutagenesis studies have identified a cluster of residues critical to fibrinogen binding in the cap subdomain of αIIb's β-propeller region (*69*, *70*) and on β3's specificity-determining loop (*9*, *71*).

The extensive area capable of encompassing these putative contacts between αIIbβ3's ectodomain and fibrinogen's γC module may well be responsible for the longevity of the integrin−fibrinogen complex. This concept is supported by our observation

(Figure S5 of the Supporting Information) of relatively slow dissociation rates, even for αIIbβ3's interactions with echistatin, a 49-residue disintegrin with a single RGD site (*47*). Echistatin's nine-residue carboxy-terminal segment may provide additional contacts that contribute to the stability of its complex with αIIbβ3, and similar mechanisms may stabilize fibrinogen binding. Indeed, we only observed rapid dissociation of αIIbβ3 from cHarGD, a monovalent cyclic peptide integrin antagonist (*72*).

Physiological Regulation of Integrin Activation. We recognize the challenges in extrapolating from a well-characterized receptor−ligand system to an environment of densely packed αIIbβ3 receptors with their extracellular domains protruding from a platelet surface, linked through transmembrane segments to distant cytoplasmic domains. Recent advances in cell biology, biochemistry, biophysics, and structural biology have demonstrated how integrin-associated proteins, especially talin and kindlins, control the receptor's activation state through interactions with β3's cytodomain, the phospholipid bilayer, and the actin cytoskeleton (*6*, *7*, *73*, *74*). Our model system is not designed to address the multiplicity of these protein−protein and protein−lipid interactions. Conversely, because cytodomain separation has emerged as a hallmark of integrin activation (*6*, *7*, *75*), our immunocapture of αIIbβ3 through its αIIb carboxy terminus may stabilize the receptor's primed conformation, replicating mechanisms that regulate binding to its primary physiological ligand, fibrinogen.

CONCLUSIONS

We demonstrated that fibrinogen's interactions with the αIIbβ3 integrin are dynamically regulated by priming-induced conformational changes in the receptor's ectodomain. Our studies with recombinant fibrinogen, coupled with structural insights, support the postulate that the stability of the integrin−fibrinogen complex depends on electrostatic interactions between an aspartate residue on the carboxy terminus of fibrinogen's γ-module and the β3 subunit's MIDAS Mg^{2+} ion. Our equilibrium and transition-state thermodynamic analyses suggest that locking the initially flexible integrin targeting segment into a binding-competent conformation requires overcoming a substantial entropy barrier. Only then can the enthalpy-favorable, long-lived integrin−fibrinogen complex be assembled. We speculate that kinetics and thermodynamics interact to localize the initiating events in hemostasis to vascular injury sites.

ACKNOWLEDGMENT

Thanks to Brian Holliday (Department of Pathology, University of North Carolina) for purification of normal and γ△408-411 recombinant fibrinogens. Thanks to Oleg V. Gorkun (Department of Pathology and Laboratory Medicine, University of North Carolina) and David A. Horita (Department of Biochemistry, Wake Forest University School of Medicine) for helpful discussions. Thanks to Julie Edelson (Office of Research and Sponsored Programs, Wake Forest University) for her editorial insights.

SUPPORTING INFORMATION AVAILABLE

Results of fitting each integrin−fibrinogen binding data set to both a single-site and a bivalent analyte model (Table S1), procedures used to validate the off rate determinations (Table S2), SPR time courses of integrin capture by mAb A4, stabilization, fibrinogen binding, dissociation, and regeneration (Figure S1), SPR fibrinogen binding profiles obtained as a function of the primed integrin capture level (Figure S2), data from solid-phase assays measuring binding of biotin-labeled fibrinogen to resting, primed, and primed and eptifibatide-blocked αIIbβ3 (Figure S3), SPR data examining concentration-dependent inhibition of binding of fibrinogen to immunocaptured, primed αIIbβ3 by eptifibatide and synthetic peptide HHLGGAKQAGDV (Figure S4), and SPR kinetics and binding modes for fibrinogen−αIIbβ3, PAC-1−αIIbβ3, αIIbβ3−echistatin, and αIIbβ3−cHarGD complexes (Figure S5). This material is available free of charge via the Internet at http://pubs.acs.org.

REFERENCES

1. Coller, B. S., and Shattil, S. J. (2008) The GPIIb/IIIa (integrin αIIbβ3) odyssey: A technology-driven saga of a receptor with twists, turns, and even a bend. *Blood 112*, 3011–3025.
2. Bennett, J. S. (2001) Platelet-fibrinogen interactions. *Ann. N.Y. Acad. Sci. 936*, 340–354.
3. Leisner, T. M., Yuan, W., DeNofrio, J. C., Liu, J., and Parise, L. V. (2007) Tickling the tails: Cytoplasmic domain proteins that regulate integrin αIIbβ3 activation. *Curr. Opin. Hematol. 14*, 255–261.
4. Ma, Y. Q., Yang, J., Pesho, M. M., Vinogradova, O., Qin, J., and Plow, E. F. (2006) Regulation of integrin αIIbβ3 activation by distinct regions of its cytoplasmic tails. *Biochemistry 45*, 6656–6662.
5. Travis, M. A., Humphries, J. D., and Humphries, M. J. (2003) An unraveling tale of how integrins are activated from within. *Trends Pharmacol. Sci. 24*, 192–197.
6. Zhu, J., Luo, B. H., Xiao, T., Zhang, C., Nishida, N., and Springer, T. A. (2008) Structure of a complete integrin ectodomain in a physiologic resting state and activation and deactivation by applied forces. *Mol. Cell 32*, 849–861.
7. Ye, F., Hu, G., Taylor, D., Ratnikov, B., Bobkov, A. A., McLean, M. A., Sligar, S. G., Taylor, K. A., and Ginsberg, M. H. (2010) Recreation of the terminal events in physiological integrin activation. *J. Cell Biol. 188*, 157–173.
8. Yang, J., Ma, Y. Q., Page, R. C., Misra, S., Plow, E. F., and Qin, J. (2009) Structure of an integrin αIIbβ3 transmembrane-cytoplasmic heterocomplex provides insight into integrin activation. *Proc. Natl. Acad. Sci. U.S.A. 106*, 17729–17734.
9. Xiao, T., Takagi, J., Coller, B. S., Wang, J. H., and Springer, T. A. (2004) Structural basis for allostery in integrins and binding to fibrinogen-mimetic therapeutics. *Nature 432*, 59–67.
10. Springer, T. A., Zhu, J., and Xiao, T. (2008) Structural basis for distinctive recognition of fibrinogen γC peptide by the platelet integrin αIIbβ3. *J. Cell Biol. 182*, 791–800.
11. Luo, B. H., Carman, C. V., and Springer, T. A. (2007) Structural basis of integrin regulation and signaling. *Annu. Rev. Immunol. 25*, 619–647.
12. Litvinov, R. I., Vilaire, G., Li, W., DeGrado, W. F., Weisel, J. W., and Bennett, J. S. (2006) Activation of individual αIIbβ3 integrin molecules by disruption of transmembrane domain interactions in the absence of clustering. *Biochemistry 45*, 4957–4964.
13. Banno, A., and Ginsberg, M. H. (2008) Integrin activation. *Biochem. Soc. Trans. 36*, 229–234.
14. Rocco, M., Rosano, C., Weisel, J. W., Horita, D. A., and Hantgan, R. R. (2008) Integrin conformational regulation: Uncoupling extension/tail separation from changes in the head region by a multiresolution approach. *Structure 16*, 954–964.
15. Hantgan, R. R., Stahle, M. C., Connor, J. H., Connor, R. F., and Mousa, S. A. (2007) αIIbβ3 priming and clustering by orally active and intravenous integrin antagonists. *J. Thromb. Haemostasis 5*, 542–550.
16. Hantgan, R. R., and Stahle, M. C. (2009) Integrin priming dynamics: Mechanisms of integrin antagonist-promoted αIIbβ3:PAC-1 molecular recognition. *Biochemistry 48*, 8355–8365.
17. Bennett, J. S., and Vilaire, G. (1979) Exposure of platelet fibrinogen receptors by ADP and epinephrine. *J. Clin. Invest. 64*, 1393–1401.
18. Faraday, N., Goldschmidt-Clermont, P., Dise, K., and Bray, P. F. (1994) Quantitation of soluble fibrinogen binding to platelets by fluorescence-activated flow cytometry. *J. Lab. Clin. Med. 123*, 728–740.
19. Xia, Z., Wong, T., Liu, Q., Kasirer-Friede, A., Brown, E., and Frojmovic, M. M. (1996) Optimally functional fluorescein isothiocyanate-labelled fibrinogen for quantitative studies of binding to activated platelets and platelet aggregation. *Br. J. Haematol. 93*, 204–214.
20. Kornecki, E., Niewiarowski, S., Morinelli, T. A., and Kloczewiak, M. (1981) Effects of chymotrypsin and adenosine diphosphate on the

exposure of fibrinogen receptors on normal human and Glanzmann's thrombasthenic platelets. *J. Biol. Chem. 256*, 5696–5701.
21. Di, M. G., Thiagarajan, P., Perussia, B., Martinez, J., Shapiro, S., Trinchieri, G., and Murphy, S. (1983) Exposure of platelet fibrinogen-binding sites by collagen, arachidonic acid, and ADP: Inhibition by a monoclonal antibody to the glycoprotein IIb-IIIa complex. *Blood 61*, 140–148.
22. Baldassare, J. J., Kahn, R. A., Knipp, M. A., and Newman, P. J. (1985) Reconstruction of platelet proteins into phospholipid vesicles. Functional proteoliposomes. *J. Clin. Invest. 75*, 35–39.
23. Phillips, D. R., and Baughan, A. K. (1983) Fibrinogen binding to human platelet plasma membranes. Identification of two steps requiring divalent cations. *J. Biol. Chem. 258*, 10240–10246.
24. Parise, L. V., and Phillips, D. R. (1985) Reconstitution of the purified platelet fibrinogen receptor. Fibrinogen binding properties of the glycoprotein IIb-IIIa complex. *J. Biol. Chem. 260*, 10698–10707.
25. Smith, J. W., Piotrowicz, R. S., and Mathis, D. (1994) A mechanism for divalent cation regulation of β3-integrins. *J. Biol. Chem. 269*, 960–967.
26. Bajt, M. L., Ginsberg, M. H., Frelinger, A. L. I., Berndt, M. C., and Loftus, J. C. (1992) A spontaneous mutation of integrin αIIbβ3 (Platelet glycoprotein IIb-IIIa) helps define a ligand binding site. *J. Biol. Chem. 267*, 3789–3794.
27. Smith, J. W., Ruggeri, Z. M., Kunicki, T. J., and Cheresh, D. A. (1990) Interaction of integrins $\alpha_V\beta_3$ and glycoprotein IIb-IIIa with fibrinogen. Differential peptide recognition accounts for distinct binding sites. *J. Biol. Chem. 265*, 12267–12271.
28. Charo, I. F., Nannizzi, L., Phillips, D. R., Hsu, M. A., and Scarborough, R. M. (1991) Inhibition of fibrinogen binding to GP IIb-IIIa by a GP IIIa peptide. *J. Biol. Chem. 266*, 1415–1421.
29. Du, X., Plow, E. F., Frelinger, A. L., III, O'Toole, T. E., Loftus, J. C., and Ginsberg, M. H. (1991) Ligands "activate" integrin $\alpha_{IIb}\beta_3$ (platelet GPIIb-IIIa). *Cell 65*, 409–416.
30. Huber, W., Hurst, J., Schlatter, D., Barner, R., Hübscher, J., Kouns, W. C., and Steiner, B. (1995) Determination of kinetic constants for the interaction between the platelet glycoprotein IIb-IIIa and fibrinogen by means of surface plasmon resonance. *Eur. J. Biochem. 227*, 647–656.
31. Hantgan, R. R., Paumi, C., Rocco, M., and Weisel, J. W. (1999) Effects of ligand-mimetic peptides Arg-Gly-Asp-X (X = Phe, Trp, Ser) on αIIbβ3 integrin conformation and oligomerization. *Biochemistry 38*, 14461–14464.
32. Muller, B., Zerwes, H. G., Tangemann, K., Peter, J., and Engel, J. (1993) Two-step binding mechanism of fibrinogen to αIIbβ3 integrin reconstituted into planar lipid bilayers. *J. Biol. Chem. 268*, 6800–6808.
33. Pesho, M. M., Bledzka, K., Michalec, L., Cierniewski, C. S., and Plow, E. F. (2006) The specificity and function of the metal binding sites in the integrin β3 A-domain. *J. Biol. Chem. 281*, 23034–23041.
34. Hantgan, R. R., Braaten, J. V., and Rocco, M. (1993) Dynamic light scattering studies of $\alpha_{IIb}\beta_3$ solution conformation. *Biochemistry 32*, 3935–3941.
35. Farrell, D. H., Thiagarajan, P., Chung, D. W., and Davie, E. W. (1992) Role of fibrinogen α and γ chain sites in platelet aggregation. *Proc. Natl. Acad. Sci. U.S.A. 89*, 10729–10732.
36. Rooney, M. M., Farrell, D. H., van Hemel, B. M., De Groot, P. G., and Lord, S. T. (1998) The contribution of the three hypothesized integrin-binding sites in fibrinogen to platelet-mediated clot retraction. *Blood 92*, 2374–2381.
37. Hawiger, J. (1995) Adhesive ends of fibrinogen and its antiadhesive peptides: The end of a saga. *Semin. Hematol. 32*, 99–109.
38. Kloczewiak, M., Timmons, S., and Hawiger, J. (1983) Recognition site for the platelet receptor is present on the 15-residue carboxy-terminal fragment of the γ chain of human fibrinogen and is not involved in the fibrin polymerization reaction. *Thromb. Res. 29*, 249–255.
39. Peerschke, E. I., Francis, C. W., and Marder, V. J. (1986) Fibrinogen binding to human blood platelets: Effect of γ chain carboxyterminal structure and length. *Blood 67*, 385–390.
40. Farrell, D. H., and Thiagarajan, P. (1994) Binding of recombinant fibrinogen mutants to platelets. *J. Biol. Chem. 269*, 226–231.
41. Rooney, M. M., Parise, L. V., and Lord, S. T. (1996) Dissecting clot retraction and platelet aggregation: Clot retraction does not require an intact fibrinogen γ chain C terminus. *J. Biol. Chem. 271*, 8553–8555.
42. Remijn, J. A., IJsseldijk, M. J., van Hemel, B. M., Galanakis, D. K., Hogan, K. A., Lounes, K. C., Lord, S. T., Sixma, J. J., and De Groot, P. G. (2002) Reduced platelet adhesion in flowing blood to fibrinogen by alterations in segment γ316−322, part of the fibrin-specific region. *Br. J. Haematol. 117*, 650–657.
43. Lounes, K. C., Ping, L., Gorkun, O. V., and Lord, S. T. (2002) Analysis of engineered fibrinogen variants suggests that an additional site mediates platelet aggregation and that "B-b" interactions have a role in protofibril formation. *Biochemistry 41*, 5291–5299.
44. Hogan, K. A., Gorkun, O. V., Lounes, K. C., Coates, A. I., Weisel, J. W., Hantgan, R. R., and Lord, S. T. (2000) Recombinant fibrinogen Vlissingen/Frankfurt IV. The deletion of residues 319 and 320 from the γ chain of firbinogen alters calcium binding, fibrin polymerization, cross-linking, and platelet aggregation. *J. Biol. Chem. 275*, 17778–17785.
45. Podolnikova, N. P., Gorkun, O. V., Loreth, R. M., Yee, V. C., Lord, S. T., and Ugarova, T. P. (2005) A cluster of basic amino acid residues in the GA 370−381 sequence of fibrinogen comprise a binding site for platelet integrin αIIbβ3 (glycoprotein IIb/IIIa). *Biochemistry 44*, 16220–16230.
46. Podolnikova, N. P., Yakubenko, V. P., Volkov, G. L., Plow, E. F., and Ugarova, T. P. (2003) Identification of a novel binding site for platelet integrins αIIbβ3 (GPIIbIIIa) and α5β1 in the γC-domain of fibrinogen. *J. Biol. Chem. 278*, 32251–32258.
47. Hantgan, R. R., Stahle, M. C., and Horita, D. A. (2008) Entropy drives integrin αIIbβ3−echistatin binding: Evidence from surface plasmon resonance spectroscopy. *Biochemistry 47*, 2884–2892.
48. Hantgan, R. R., and Hermans, J. (1979) Assembly of fibrin: A light scattering study. *J. Biol. Chem. 254*, 11272–11281.
49. Gorkun, O. V., Veklich, Y. I., Weisel, J. W., and Lord, S. T. (1997) The conversion of fibrinogen to fibrin: Recombinant fibrinogen typifies plasma fibrinogen. *Blood 89*, 4407–4414.
50. Day, Y. S., Baird, C. L., Rich, R. L., and Myszka, D. G. (2002) Direct comparison of binding equilibrium, thermodynamic, and rate constants determined by surface- and solution-based biophysical methods. *Protein Sci. 11*, 1017–1025.
51. Phillips, D. R., and Scarborough, R. M. (1997) Clinical pharmacology of eptifibatide. *Am. J. Cardiol. 80*, 11B–20B.
52. Hantgan, R. R., Rocco, M., Nagaswami, C., and Weisel, J. W. (2001) Binding of a fibrinogen mimetic stabilizes integrin αIIbβ3's open conformation. *Protein Sci. 10*, 1614–1626.
53. Hettasch, J. M., Bolyard, M. G., and Lord, S. T. (1992) The residues AGDV of recombinant γ chains of human fibrinogen must be carboxy-terminal to support human platelet aggregation. *Thromb. Haemostasis 68*, 701–706.
54. Liu, Q. D., Rooney, M. M., Kasirerfriede, A., Brown, E., Lord, S. T., and Frojmovic, M. M. (1998) Role of the γ chain Ala-Gly-Asp-Val and Aα chain Arg-Gly-Asp-Ser sites of fibrinogen in coaggregation of platelets and fibrinogen-coated beads. *Biochim. Biophys. Acta 1385*, 33–42.
55. Kloczewiak, M., Timmons, S., Lukas, T. J., and Hawiger, J. (1984) Platelet receptor recognition site on human fibrinogen. synthesis and structure-function relationships of peptides corresponding to the carboxy-terminal segment of the γ chain. *Biochemistry 23*, 1767–1774.
56. Winzor, D. J., and Jackson, C. M. (2005) Interpretation of the temperature dependence of rate constants in biosensor studies. *Anal. Biochem. 337*, 289–293.
57. Glasstone, S., Laidler, K. J., and Eyring, H. (1941) Reactions in Solution. In The Theory of Rate Processes (Glasstone, S., Laidler, K. J., and Eyring, H., Eds.) pp 400−476, McGraw-Hill Book Co., New York.
58. Hantgan, R. R., Lyles, D. S., Mallett, T. C., Rocco, M., Nagaswami, C., and Weisel, J. W. (2003) Ligand Binding Promotes the Entropy-Driven Oligomerization of Integrin αIIbβ3. *J. Biol. Chem. 278*, 3417–3426.
59. Chen, J., Salas, A., and Springer, T. A. (2003) Bistable regulation of integrin adhesiveness by a bipolar metal ion cluster. *Nat. Struct. Biol. 10*, 995–1001.
60. Lee, K. K., Fitch, C. A., and Garcia-Moreno, E. B. (2002) Distance dependence and salt sensitivity of pairwise, coulombic interactions in a protein. *Protein Sci. 11*, 1004–1016.
61. Kodandapani, R., Veerapandian, B., Kunicki, T. J., and Ely, K. R. (1995) Crystal structure of the OPG2 Fab. An antireceptor antibody that mimics an RGD cell adhesion site. *J. Biol. Chem. 270*, 2268–2273.
62. Abrams, C. S., Ruggeri, Z. M., Taub, R., Hoxie, J. A., Nagaswami, C., Weisel, J. W., and Shattil, S. J. (1992) Anti-idiotypic antibodies against an antibody to the platelet glycoprotein (GP) IIb-IIIa complex mimic GP IIb-IIIa by recognizing fibrinogen. *J. Biol. Chem. 267*, 2775–2785.
63. Kollman, J. M., Pandi, L., Sawaya, M. R., Riley, M., and Doolittle, R. F. (2009) Crystal structure of human fibrinogen. *Biochemistry 48*, 3877–3886.
64. Everse, S. J., Spraggon, G., Veerapandian, L., Riley, M., and Doolittle, R. F. (1998) Crystal structure of fragment double-D from

human fibrin with two different bound ligands. *Biochemistry 37*, 8637–8642.
65. Kostelansky, M. S., Betts, L., Gorkun, O. V., and Lord, S. T. (2002) 2.8 Å Crystal Structures of Recombinant Fragment D with and without Two Peptide Ligands: GHRP binding to the "b" site disrupts its nearby calcium binding site. *Biochemistry 41*, 12124–12132.
66. Yang, Z., Kollman, J. M., Pandi, L., and Doolittle, R. F. (2001) Crystal structure of native chicken fibrinogen at 2.7 Å resolution. *Biochemistry 40*, 12515–12523.
67. Cunningham, B. C., and Wells, J. A. (1993) Comparison of a structural and a functional epitope. *J. Mol. Biol. 234*, 554–563.
68. Duan, J., Wu, J., Valencia, C. A., and Liu, R. (2007) Fibronectin type III domain based monobody with high avidity. *Biochemistry 46*, 12656–12664.
69. Puzon-McLaughlin, W., Kamata, T., and Takada, Y. (2000) Multiple discontinuous ligand-mimetic antibody binding sites define a ligand binding pocket in integrin αIIbβ3. *J. Biol. Chem. 275*, 7795–7802.
70. Kamata, T., Tieu, K. K., Irie, A., Springer, T. A., and Takada, Y. (2001) Amino acid residues in the αIIb subunit that are critical for ligand binding to integrin αIIbβ3 are clustered in the β-propeller model. *J. Biol. Chem. 276*, 44275–44283.
71. Artoni, A., Li, J., Mitchell, B., Ruan, J., Takagi, J., Springer, T. A., French, D. L., and Coller, B. S. (2004) Integrin β3 regions controlling binding of murine mAb 7E3: Implications for the mechanism of integrin αIIbβ3 activation. *Proc. Natl. Acad. Sci. U.S.A. 109*, 3725–3723.
72. Hantgan, R. R., Dutta, S., and Guthold, M. (2009) Unraveling Integrin Antagonists' Target-Recognition Mechanisms. *Biophys. J. 96* (Suppl.), 600A.
73. Anthis, N. J., Wegener, K. L., Ye, F., Kim, C., Goult, B. T., Lowe, E. D., Vakonakis, I., Bate, N., Critchley, D. R., Ginsberg, M. H., and Campbell, I. D. (2009) The structure of an integrin/talin complex reveals the basis of inside-out signal transduction. *EMBO J. 28*, 3623–3632.
74. Yang, J., Ma, Y. Q., Page, R. C., Misra, S., Plow, E. F., and Qin, J. (2009) Structure of an integrin αIIbβ3 transmembrane-cytoplasmic heterocomplex provides insight into integrin activation. *Proc. Natl. Acad. Sci. U.S.A. 106*, 17729–17734.
75. Askari, J. A., Tynan, C. J., Webb, S. E., Martin-Fernandez, M. L., Ballestrem, C., and Humphries, M. J. (2010) Focal adhesions are sites of integrin extension. *J. Cell Biol. 188*, 891–903.
76. DeLano, W. L. (2002) The PyMOL Molecular Graphics System, DeLano Scientific, San Carlos, CA.